



**1 Influence of intra-event rainfall variation on surface–subsurface flow**  
**2 generation and soil loss under different surface covers by long-term**  
**3 field observations**

4 Jian Duan<sup>a\*</sup>, Hai-Jin Zheng<sup>a</sup>, Yao-Jun Liu<sup>b</sup>, Ming-Hao Mo<sup>a</sup>, Yue-Jun Song<sup>a</sup>, Jie Yang<sup>a</sup>

5 <sup>a</sup> *Jiangxi Provincial Key Laboratory of Soil Erosion and Prevention, Jiangxi Academy of Water*

6 *Science and Engineering, Nanchang, Jiangxi 330029, China*

7 <sup>b</sup> *School of Geographic Sciences, Hunan Normal University, Changsha, 410081, China*

8 **\* Corresponding author:**

9 Jian Duan

10 Institute of Soil and Water Conservation,

11 Jiangxi Academy of Water Science and Engineering,

12 Nanchang, Jiangxi 330029, China.

13 E-mail: [djlynn20@126.com](mailto:djlynn20@126.com)

14 Tel: + +86-0791-87606870

15 Fax: +86-0791-87606699



**Abstract:** Rainfall is the main driver of runoff generation and soil erosion. The impacts of natural rainfall on water erosion have been extensively studied at an inter-event scale; however, very few studies have explored the intra-event influences and associated responses to different surface cover types. In this study, long-term in situ field observations of surface runoff, subsurface flow, and soil loss characteristics in three surface cover plots (bare land, litter and grass cover) under natural rainfall events were conducted from 2002 to 2012 in the red soil hilly region of southern China. According to the period of most concentrated rainfall, 262 rainfall events were classified into four types of intra-event variation: advanced, intermediate, delayed, and uniform patterns. For bare land, the advanced pattern with the shortest duration and the highest intensity was main rainfall type for surface runoff and soil loss; the contribution rates were 57.24% and 75.17% for surface runoff and soil loss, respectively. Sediment yields were more sensitive to intra-event rainfall variation than surface runoff. The highest subsurface flow was found in the delayed pattern with the longest duration and high depth, followed by the uniform, intermediate, and advanced patterns. For all rainfall patterns, compared to the bare land, surface cover significantly reduced surface runoff and soil erosion by 88.01 to 91.69% and by 97.80 to 97.95%, respectively, while subsurface flow was increased from 3.55 to 5.92 times. The reduction benefits of litter cover were comparable to those of grass cover. However, the increasing benefit of subsurface flow for litter cover for each rainfall pattern ranged from 1.38 to 2.67 times those of grass cover. Moreover, surface cover weakened the influences of intra-event rainfall variation on surface-subsurface flow and soil loss. The results demonstrated that intra-event rainfall variation had important effects on surface-subsurface flow and soil loss, and provided a basis for optimizing surface cover measures to effectively respond to extreme water erosion and drought caused by global climate change.



38 **Keywords:** subsurface flow; rainfall intensity fluctuation; surface runoff; soil erosion; natural  
39 rainfall; surface cover

## 40 **1 Introduction**

41 Soil is a crucial natural resource for life on Earth, similar to water and air. Soil offers a wide range  
42 of services and products, especially ones on those that support biodiversity, water cycling, soil  
43 conservation, carbon sequestration, and ecosystem productivity. Soil degradation is becoming a  
44 highly serious risk to land productivity and human well-being (Pimentel et al., 1976; Montanarella  
45 et al., 2016). A major cause of soil degradation is water erosion, resulting in losses in topsoil and  
46 nutrients (Poesen, 2018; Tsymbarovich et al., 2020). Numerous investigations have noted a  
47 decline in soil quality in various regions throughout the world. This decline helps to explain why  
48 production costs are increasing, crop yields are declining, and farmland is even being abandoned  
49 in worst-case scenarios (Montgomery, 2007; García-Ruiz et al., 2015). According to the Food and  
50 Agriculture Organization (FAO)-led Global Soil Partnership, 75 billion tons of soil is lost from  
51 agricultural lands globally each year, causing an estimated \$400 billion in annual economic losses  
52 (GSP, 2017).

53 Rainfall is the main driver of runoff generation and soil erosion. Inter-event rainfall variables,  
54 such as total rainfall amount (RA), rainfall duration (RD), average intensity (I), and maximum  
55 30-min intensity (I30) are frequently utilized to evaluate the impacts of inter-event rainfall  
56 characteristic variability on runoff and soil erosion (Hammad et al., 2006). Some researches  
57 employ rainfall amount, rainfall duration, and rainfall intensity (I30) as indicators to translate  
58 rainfall events into distinct rainfall regimes, such as long-duration/light-intensity and  
59 short-duration/heavy-intensity regimes, to explore water erosion characteristics (Wei et al., 2007;



60 [Fang et al., 2012](#)). These rainfall parameters, however, do not account for intra-event variability  
61 characteristics in natural rainfall features, such as the temporal distributions of intensity peaks in  
62 rainfall profiles ([Flanagan et al., 1988](#)), which have important impacts on water erosion and  
63 related landsurface processes ([Dunkerley, 2012](#); [An et al., 2022](#); [Liu et al., 2022](#)). For example,  
64 rainfall events with the same features (e.g., RA, RD, I, and I30) create significantly different  
65 runoff rates and soil losses, and these phenomena may be caused by intra-fluctuations in rainfall  
66 characteristics ([Todisco, 2014](#); [Mohamadi and Kavian, 2015](#); [Almeida et al., 2021](#)). Therefore,  
67 there is a strong need to incorporate intra-event rainfall variability when studying rainfall  
68 infiltration, runoff generation, and soil erosion ([Dunkerley, 2012](#); [Dunkerley, 2021b](#)).  
69 Numerous studies have shown that intra-event rainfall variability have significantly impacts on the  
70 processes of soil erosion, particularly on runoff, soil loss, and particle dispersion ([Zhang et al.,](#)  
71 [1997](#); [Parsons and Stone, 2006](#); [An et al., 2014](#); [Wang et al., 2017](#)). The results of previous studies  
72 have largely been obtained based on simulated rainfall experiments. For example, the rainfall  
73 duration is generalized into three equal periods, and combinations of different rainfall intensities  
74 are designed by tuning several intensity peaks to simulate rainfall intensity patterns, such as  
75 increasing, decreasing, rising-falling, falling-rising and constant patterns ([Wang et al., 2017](#);  
76 [Alavinia et al., 2019](#); [Macedo et al., 2021](#)). However, the simplified synthesis approach may not  
77 adequately capture the complexities of intra-fluctuation in natural rainfall ([Wang et al., 2016](#);  
78 [Macedo et al., 2021](#); [Liu et al., 2022](#)). Natural rainfall events are notable for their continually  
79 variable intensities, making it difficult to extend previous research based on simulated rainfall  
80 conditions to natural rainfall conditions. Due to the lack of high temporal resolution data in natural  
81 rainfall from long-term observations, previous studies cannot accurately reveal the runoff and



erosion differences caused by intra-event rainfall variability. Furthermore, most of the existing research focuses on the impacts of inter- and intra-event rainfall differences on surface runoff and soil erosion (Parsons and Stone, 2006; Wang et al., 2017; Alavinia et al., 2019), and little attention is given to the response of subsurface flow generation. Subsurface flow is a key component of rainfall runoff, and its output is even higher than that of surface runoff in the rainfall regime with long duration and high depth (Liu et al., 2016; Duan et al., 2017). The formation of subsurface flow altered soil moisture redistribution, soil hydrology and slope erosion processes (Zheng et al., 2004; An et al., 2021). The knowledge gaps impede a better understanding of soil hydrological processes and erosion mechanisms caused by natural rainfall.

To reduce water erosion, mulching with litter or living plants is widely used around the world to increase surface coverage (Shi et al., 2012; Duan et al., 2022). Surface cover with litter or living plants effectively reduces the kinetic energy of raindrops and protects the soil surface from raindrop splashing. On the other hand, surface cover roughens the surface and causes overland flow tortuosity, which boosts infiltration and lessens water erosion (Nearing et al., 2005). The essential roles of surface cover in promoting rainfall infiltration and reducing surface runoff and soil loss have received widespread attention and positive evaluation, but little attention has been paid to the role of surface cover in regulating surface-subsurface flow and soil loss under different intra-event rainfall variations. As a result, a scientific assessment of the effects of surface cover on surface-subsurface flow and soil erosion under intra-event rainfall variations are critical for watershed flood prediction and forecasting, soil erosion, and hydrological cycle computation.

By considering the above knowledge gaps, in this study, long-term in situ field observations of surface-subsurface flow and soil loss were conducted in the red soil hilly region of southern China



104 from 2002 to 2012 for three surface cover types (bare land, litter and grass cover) under natural  
105 rainfall conditions. Based on rainfall data with a 1-min temporal resolution, 262 rainfall events  
106 over 11 consecutive years were selected and classified into four types of intra-event rainfall  
107 variation including advanced, intermediate, delayed, and uniform. The purpose of this study was  
108 to (1) investigate whether intra-event rainfall variability influences surface-subsurface flow and  
109 soil loss under natural rainfall conditions; (2) explore the effects of different surface cover types  
110 on surface-subsurface flow and soil loss, and (3) determine the role of surface cover in regulating  
111 surface-subsurface flow generation and soil loss for intra-event rainfall variation.

## 112 **2 Materials and Methods**

### 113 *2.1 Study area*

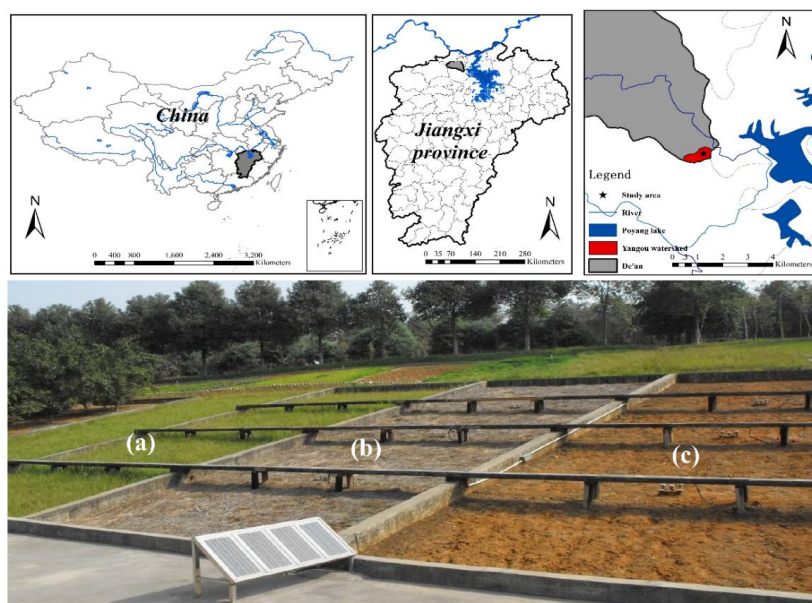
114 The red soil hilly regions are located in the tropical and subtropical regions of China, with a total  
115 area of 1.18 million km<sup>2</sup>. This region is an important agricultural area for tropical and subtropical  
116 fruits, cash and food crops in China. However, the region has experienced severe water erosion  
117 due to intense rainstorms, the hilly terrain and unsustainable human activities (Duan et al., 2022).

118 Many vegetation restoration projects have been implemented since the 1980s. Surface cover with  
119 living grass and litter is an effective technique to prevent water erosion, and it is widely used for  
120 soil and water conservation efforts. The eroded area and degree were effectively controlled in this  
121 region.

122 The study was conducted in the Jiangxi Eco-Science Park of Soil and Water Conservation, which  
123 is located in the Yangou catchment (29°16' N to 29°17' N, 115°42' E to 115°43' E), 15 km away  
124 from the largest freshwater lake (Poyang Lake) in Jiangxi Province, southern China (Fig. 1). The  
125 catchment has a subtropical humid monsoon climate with an average annual precipitation of 1469



126 mm. The rainfall distribution is uneven throughout the year, with approximately 70% or more of  
 127 the total precipitation falling between spring and summer (from March to August). The altitude of  
 128 this area ranges from 30 m to 90 m, and the mean annual temperature is approximately 16.7 °C.



129  
 130 **Fig. 1** Location of the study area and the photos of three types of runoff plots including grass  
 131 cover (a), litter cover (b) and bare land (c).

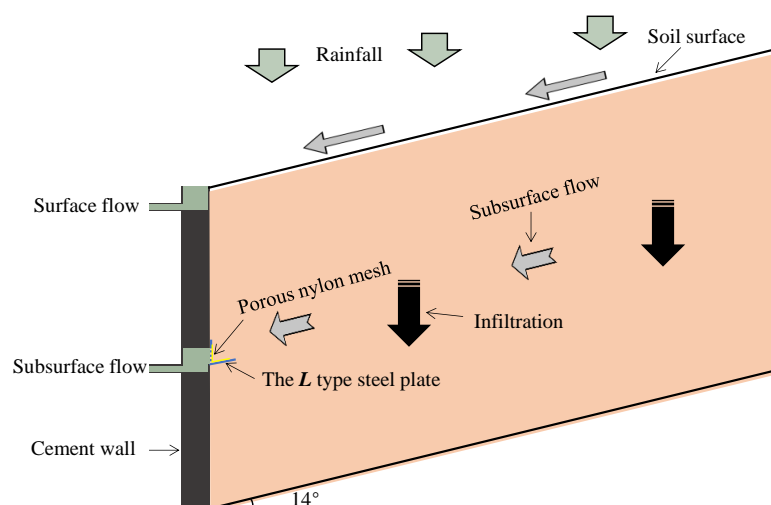
132 The dominant soil type of the region is red clay soil, which is formed by the decomposition of  
 133 Quaternary sediments. Red clay soil is classified as Ultisol in the USDA soil taxonomy system,  
 134 and it is vulnerable to water erosion. This soil has a texture composed of  $11.54 \pm 1.21\%$  sand  
 135 ( $2-0.05$  mm),  $68.06 \pm 0.15\%$  silt ( $0.05-0.002$  mm), and  $20.41 \pm 1.19\%$  clay ( $<0.002$  mm). The soil  
 136 thickness typically exceeds 100 cm, and the soil profile type is Ah-Bs-Cs according to Soil  
 137 Taxonomy (Liu et al., 2016; Ma et al., 2022a). The soil physicochemical properties vary  
 138 considerably among the different layers, especially regarding soil porosity and water infiltration  
 139 capacity. The topsoil layer (Ah) is typically 30 cm, and it is susceptible to severe soil erosion  
 140 because of its loose structure ( $1.27 \pm 0.10$  g cm<sup>-3</sup>) and the high precipitation in this region. The



141 depth of the Bs layer is 30-60 cm with a compact structure ( $1.42 \pm 0.08 \text{ g cm}^{-3}$ ) and low  
 142 permeability. The soil below 60 cm is defined as the Cs layer (parent material) with a tight  
 143 structure ( $1.53 \pm 0.07 \text{ g cm}^{-3}$ ) and poor permeability.

## 144 2.2 Plot construction

145 Three in-situ runoff plots with a size of 15 m  $\times$  5 m (length  $\times$  width) were built on an open  
 146 south-facing hillslope. Since soil erosion originates mainly from steep slopes in the red soil hilly  
 147 regions, the runoff plots were set to a fixed slope of  $14^\circ$  based on field observations. The adjacent  
 148 plots were isolated by 100 cm high concrete walls to prevent hydrological interference. Different  
 149 soil layers are responsive to hydrological processes, such as surface and subsurface flow under  
 150 natural rainfall events. To accurately measure the subsurface flow, a L-type steel plates with a gap  
 151 of 5 cm gaps were set up at a depth of 60 cm (Fig. 2). Porous nylon gauze was used to separate the  
 152 soil from the steel plates. A concrete wall was constructed outside the steel plates and a certain  
 153 area was left below the plates as a trench, which was connected to a container through a plastic  
 154 pipe to collect runoff and sediment produced from natural rainfall events.



155





156 **Fig. 2** Schematic diagrams of the runoff plot and the surface-subsurface flow and sediment  
157 collection system.

### 158 2.3 Experimental design

159 In this study, the field experiment included three surface cover types: bare land, grass cover and  
160 litter cover. Bare land was used as a control treatment and weeds were manually removed from the  
161 runoff plots every two months without tillage and loosening. The grass species planted in the grass  
162 cover plot was *Paspalum natatum* Flugge, which is a quickly growing perennial grass that can be  
163 used extensively to reduce runoff and soil erosion. Grass seeds were evenly spread at a density of  
164 20 g m<sup>-2</sup> in the grass cover plots after runoff plot construction. Grass growth was completely  
165 dependent on natural rainfall without human interference, such as fertilization, irrigation,  
166 reseeding, and cutting, during the study period. For the litter cover plot, a 5-cm thick layer of litter  
167 was placed on the soil surface to reduce water erosion. The litter was supplied from cutting *P.*  
168 *natatum* and was replenished quarterly throughout the decade.

### 169 2.4 In situ observation

170 Surface runoff, subsurface flow, and soil loss data were collected and measured for each runoff  
171 plot after each natural rainfall event during the study period. Five measurements were taken using  
172 a straightedge and the average value was used to represent the water depth. The runoff volume for  
173 each rainfall event was calculated by multiplying the container water depth by its base area, and  
174 the runoff depth was measured by dividing the runoff volume by the plot area. Then a depth  
175 profile sediment sampler was used to sample runoff samples mixed with eroded materials in a  
176 surface runoff container (Wang et al., 2016). The sediment concentration was analyzed by oven  
177 drying at 105 °C to a constant weight in the laboratory. The soil loss amount was obtained by  
178 calculating the product of the runoff volume and the corresponding sediment concentration. By



179 considering the hysteresis of subsurface flow, successive rainfall events were separated into two  
180 events when the rainfall intermittent intervals exceeded 12 hours (Liu et al., 2016; Duan et al.,  
181 2017). Rainfall event temporal profiles were automatically recorded at 1-min intervals by a  
182 meteorological station with a resolution of 0.2 mm near the runoff plots.

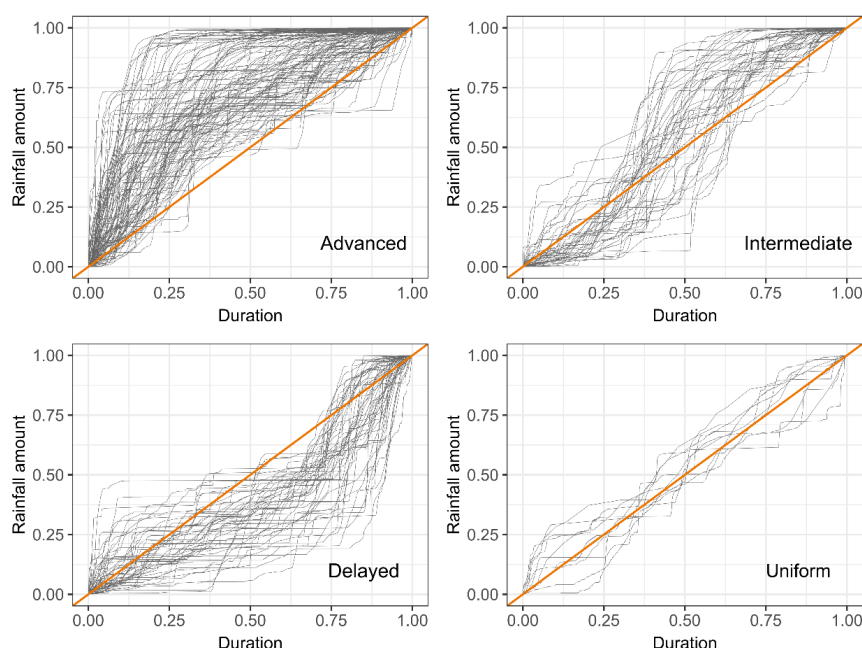
### 183 *2.5 Rainfall classification based on intra-event variation*

184 Intra-event rainfall variation classification is important for accurately describing the time-varying  
185 intensities that comprise a rainfall event (Dunkerley, 2021; Liu et al., 2022). The classification  
186 refers to the overall form of a rainfall event, for example, whether the rainfall exhibits intensity  
187 peaks in the early or late stages of an event. The application of this classification has a  
188 considerable history. Huff (1967) introduced the classification of intra-event rainfall based on  
189 quartiles. Specifically, according to which quarter of the event duration received the greatest  
190 rainfall depth, the intra-event rainfall was divided into "first quartile", "second quartile", "third  
191 quartile", and "fourth quartile" events.

192 In this paper, rainfall events were classified into four types of intra-event rainfall by the following  
193 steps (Fig. 3). Firstly, the instantaneous rainfall amount and duration are divided by the total  
194 rainfall and duration, respectively, and transformed into dimensionless parameters from 0 to 1.  
195 Secondly, the dimensionless rainfall duration was divided into three equal parts, and the  
196 cumulative rainfall was calculated for each equal time period. Finally, the intra-event rainfall  
197 patterns were defined according to the location where the maximum accumulated rainfall. Equally,  
198 rainfall events with more than 40% of the rainfall amount concentrated in the first, second and last  
199 third periods were defined as advanced, intermediate, and delayed patterns, respectively. The  
200 remaining events without obvious peaks and rainfall distributing uniformly over the duration were



201 regarded as uniform pattern (Mohamadi and Kavian, 2015; Wang et al., 2016).



202  
 203 **Fig. 3** Cumulative dimensionless curves of natural rainfall events for advanced, intermediate,  
 204 delayed, and uniform patterns, respectively.

## 205 2.6 Data analysis

206 All runoff plot construction and experimental design were completed in 2000, and the in situ  
 207 observations of surface runoff, subsurface flow and sediment from natural rainfall events have  
 208 been conducted since 2001. To reduce the disturbance of plots construction on the study results,  
 209 the observation data from 2002 to 2012 were selected to analyze the surface-subsurface flow and  
 210 soil loss characteristics under different surface cover types. Three variables, surface runoff  
 211 coefficient (*ROC*), subsurface flow rate (*SSL*), and soil loss rate (*SLR*) were employed to  
 212 characterize the effect of intra-event rainfall patterns on water erosion. The *ROC* (%), *SSL* (L  
 213 mm<sup>-1</sup>), and *SLR* (t km<sup>-2</sup> mm<sup>-1</sup>) were calculated using the following equations:

$$214 \quad ROC = \frac{SRD}{PD} \times 100\% \quad (1)$$



$$215 \quad SSL = \frac{SFV}{PD} \quad (2)$$

$$216 \quad SLR = \frac{SLA}{A \times PD} \quad (3)$$

217 where *SRD* was the surface runoff depth (mm), *SFV* was the subsurface flow volume (L), *SLA* was  
 218 the sediment loss amount (g), *PD* was the precipitation depth (mm), and *A* was the and runoff plot  
 219 area (m<sup>2</sup>).

220 Two-way analysis of variance (ANOVA) was used to assess the effects of intra-event rainfall  
 221 patterns, surface cover types and their interactions on *ROC*, *SSL*, and *SLR*. All statistical tests and  
 222 graphics were performed in R software v.4.1.3.

### 223 3 Results

#### 224 3.1 Intra-event rainfall variability

225 During the observation period, 226 natural rainfall events from 2002 to 2012 that generated runoff  
 226 and soil erosion were recorded. The rainfall events were classified into four groups (advanced,  
 227 intermediate, delayed and uniform) based on rainfall profiles (Fig. 3 and Table 1). Clearly, the  
 228 prevalence of advanced pattern in the study area accounted for 48.23% of the total erosive rainfall  
 229 events. The uniform pattern had the least probability of occurrence at 5.31%. The intermediate and  
 230 delayed patterns had comparable probabilities of occurrence at 21.24% and 25.22%, respectively.

231 As shown in Table 1, the statistical characteristics of each intra-event pattern showed an increase  
 232 in the average duration and a decrease in the average I30 values, from the advanced to the  
 233 intermediate to the delayed to the uniform pattern. The advanced pattern was characterized by the  
 234 shortest duration (732 min) and the highest intensity (8.8 mm h<sup>-1</sup>). The intermediate pattern had a  
 235 moderate duration (978 min) and moderate intensity (6.0 mm h<sup>-1</sup>). The delayed pattern included  
 236 rainfall events that had the longest duration (1409 min) and moderate intensity (6.1 mm h<sup>-1</sup>). The



uniform pattern was a cluster of rainfall events that had long duration (1362 min) and the lowest intensity ( $2.9 \text{ mm h}^{-1}$ ). The average rainfall amounts for different intra-event rainfall patterns were ranked in the order of delayed > intermediate > advanced > uniform.

**Table 1**

Rainfall eigenvalues of four intra-event rainfall patterns (IRP). D, P, and  $I_{30}$  refer to rainfall duration, depth and maximum rainfall intensity in 30 min.

RIP	Eigenvalue	Min	Max	Mean	SD	Variation	Sum	Frequency
Advanced	D (min)	27	4319	732	768	1.05	79761	109
	P (mm)	4.6	130.9	23.2	19.3	0.83	2523.5	
	$I_{30}$ ( $\text{mm h}^{-1}$ )	1.0	45.3	8.8	8.6	0.98		
Intermediate	D (min)	22	2972	978	726	0.74	46965	48
	P (mm)	7.1	72.1	26.2	17.3	0.66	1259.8	
	$I_{30}$ ( $\text{mm h}^{-1}$ )	0.9	22.9	6.0	4.6	0.77		
Delayed	D (min)	100	6191	1409	1025	0.73	80311	57
	P (mm)	8.5	129.3	30.8	22.7	0.74	1755.6	
	$I_{30}$ ( $\text{mm h}^{-1}$ )	1.0	51.2	6.1	7.3	1.20		
Uniform	D (min)	426	2460	1362	584	0.43	16343	12
	P (mm)	11.7	43.5	21.4	9.9	0.46	257.0	
	$I_{30}$ ( $\text{mm h}^{-1}$ )	1.0	5.7	2.9	1.4	0.48		

Fig. 4 shows the percentage and frequency distribution of four rainfall patterns under different rainfall durations. In each duration group, there were 33, 34, 39, 66, 48, 6 rainfall events that lasted up to 3, 3-6, 6-12, 12-24, 24-48, and more than 48 hours, respectively (Fig. 4b). This finding suggested that the rainfall events with long duration and high amount dominated in the study area. As shown in Fig. 4a, the percentage of the advanced pattern decreased from 81.82% to 31.33% as the rainfall duration increased, whereas that for the delayed pattern increased from 6.06% to 50.00%. These findings indicated that the rainfall events with short duration were dominated by advanced patterns, while the events with long duration were related to the peak intensity in the later stage (delayed pattern).

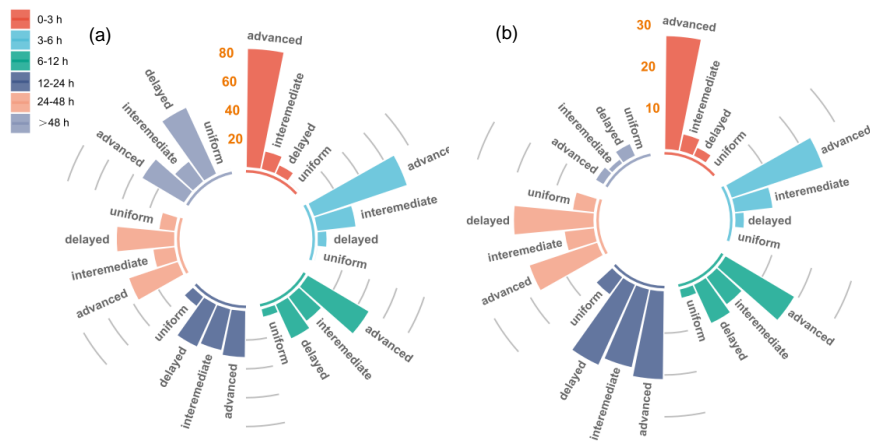


**Fig. 4** The percentage distribution (a) and frequencies (b) of intra-event rainfall patterns for different duration groups: up to 3, 3-6, 6-12, 12-24, 24-48, and more than 48 hours.

### 3.2 Surface runoff generation

Fig. 5 shows the variation in the surface runoff coefficient (ROC) under the three surface cover types for different intra-event rainfall patterns. Significant differences among the three surface cover types were observed in the ROC ( $p < 0.001$ ). For any rainfall pattern, the ROC was significantly higher in the bare land plot (15.83%) than in the litter cover plot (1.73%), and the grass cover plot (1.17%). Likewise, the ROC varied significantly among the intra-event rainfall patterns ( $p < 0.05$ ). For bare land, the average ROC was the highest in the advanced pattern (22.13%), followed by the delayed pattern (17.13%), the intermediate pattern (14.91%), and the uniform pattern (9.13%). When bare soil was covered with litter or planting grass, no obvious differences were observed among the rainfall patterns. The values ranged from 1.61% to 1.94% in the litter cover plot and from 1.08% to 1.23% in the grass cover plot. Meanwhile, for surface runoff production, there were significant interactions between intra-event rainfall patterns and surface cover types ( $p < 0.01$ ).

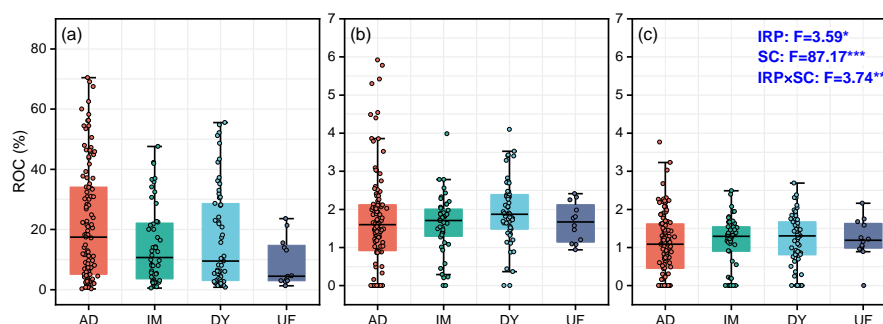


**Fig. 5** Surface runoff coefficient (ROC) under different intra-event rainfall patterns (IRP) for bare land (a), litter cover (b) and grass cover (c) plots. Displaying F values from two-way ANOVA tests for the effects of IRP and surface cover types (SC), and their interactions (IRP×SC) on ROC (\* $p < 0.05$ , \*\* $p < 0.01$  and \*\*\* $p < 0.001$ ). AD, IM, DY, and UF refer to advanced, intermediate, delayed, and uniform patterns, respectively.

### 3.3 Subsurface flow

The subsurface flow rates (SSLs) for the three surface cover types under different intra-event rainfall patterns are shown in Fig. 6. The subsurface flow under the three surface cover types were inconsistent with the surface flow. For each rainfall pattern, the lowest SSL was found in the bare land plot ( $0.46 \text{ L mm}^{-1}$ ), followed by the grass cover plot ( $1.98 \text{ L mm}^{-1}$ ) and the litter cover plot ( $2.98 \text{ L mm}^{-1}$ ). The subsurface flows for the litter cover and the grass cover were significantly higher compared to the control bare land ( $p < 0.001$ ). From the rainfall patterns, the subsurface flow rate for the bare land decreased in the order of delayed pattern ( $0.63 \text{ L mm}^{-1}$ ) > uniform pattern ( $0.50 \text{ L mm}^{-1}$ ) > intermediate pattern ( $0.44 \text{ L mm}^{-1}$ ) > advanced pattern ( $0.29 \text{ L mm}^{-1}$ ). For the litter cover, the SSL values differed slightly and ranged between  $2.93$  and  $3.13 \text{ L mm}^{-1}$  under different intra-event rainfall patterns. The SSL for grass cover was lower than that for litter cover, and the SSL values decreased in the order of delayed pattern ( $2.44 \text{ L mm}^{-1}$ ) > intermediate pattern ( $2.22 \text{ L mm}^{-1}$ ) > advanced pattern ( $1.87 \text{ L mm}^{-1}$ ) > uniform pattern ( $1.41 \text{ L mm}^{-1}$ ).

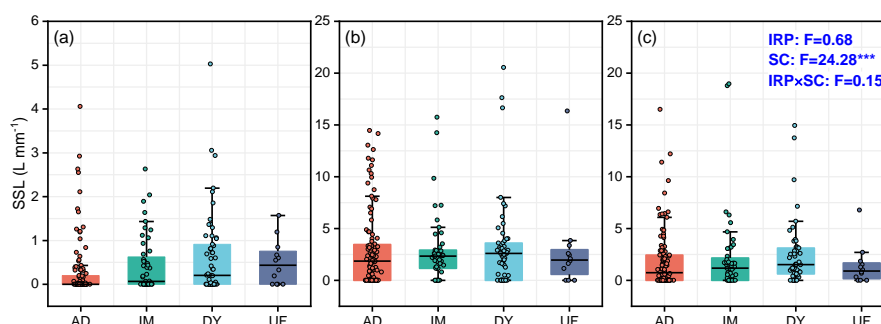


**Fig. 6** Subsurface flow rate (SSL) under the four intra-event rainfall patterns (IRP) for bare land (a), litter cover (b) and grass cover (c) plots. Displaying F values from two-way ANOVA tests for the effects of IRP, surface cover types (SC), and their interactions (IRP×SC) on SSL (\* $p < 0.05$ , \*\* $p < 0.01$  and \*\*\* $p < 0.001$ ). AD, IM, DY, and UF refer to advanced, intermediate, delayed, and uniform patterns, respectively.

### 3.4 Sediment yield

As shown in Fig. 7, the soil loss rate (SLR) of the litter cover and grass cover decreased drastically compared to that of the bare land. The SLR for the bare land was the highest ( $2.18 \text{ t km}^{-2}$ ), being 213 and 253 times greater than the SLRs for the litter cover and grass cover, respectively. The results were consistent with the surface flow of the three surface cover types. Significant differences in the SLR were identified between the intra-event rainfall patterns ( $p < 0.001$ ). The highest SLR for bare land was observed in the advanced pattern ( $5.14 \text{ t km}^{-2}$ ), with values that were 2.52, 3.68 and 39.78 times more than those of delayed, intermediate, and uniform patterns, respectively. Compared with the bare land, the SLR differences among the rainfall patterns decreased sharply for the litter cover and grass cover, with values ranging from 0.009 to  $0.013 \text{ t km}^{-2}$  and from 0.005 to  $0.011 \text{ t km}^{-2}$ , respectively. Consistent with the surface runoff, significant interactions between intra-event rainfall patterns and surface cover types were observed in the soil loss rate ( $p < 0.001$ ).



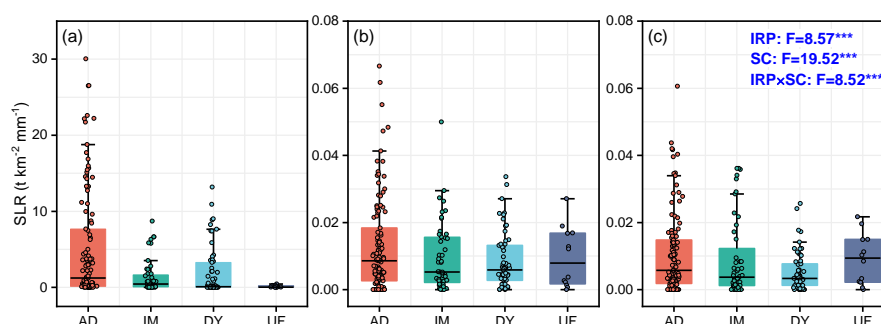


**Fig. 7** Soil loss rate (SLR) under different intra-event rainfall patterns (IRP) for bare land (a), litter cover (b) and grass cover (c) plots. Displaying F values from two-way ANOVA tests for the effects of IRP, surface cover types (SC), and their interactions (IRP×SC) on SLR (\* $p < 0.05$ , \*\* $p < 0.01$  and \*\*\* $p < 0.001$ ). AD, IM, DY, and UF refer to advanced, intermediate, delayed, and uniform patterns, respectively.

## 4 Discussion

### 4.1 Effects of intra-event rainfall variation on runoff generation and soil loss

In addition to inter-event rainfall variation, the intra-event variation significantly alters rainfall infiltration, runoff generation and erosion processes (Dunkerley, 2021; An et al., 2022). Classification based on rainfall profiles is important for describing intra-event rainfall variation. This classification is the basis for accurately elucidating the mechanisms of rainfall characteristics on water erosion (Parsons and Stone, 2006; Dunkerley, 2021). In this study, according to the occurrence period of the maximum rainfall amount, four intra-event rainfall types were classified based on 1-minute interval rainfall data from 12 consecutive years of long-term in situ observations (262 events). As shown in Table 1, the advanced and delayed patterns were characterized by short duration/heavy intensity and long duration/high amount, respectively. These two rainfall patterns were the dominant events in the study area, accounting for 73.45% of the total erosive rainfall events. The study area has a subtropical humid monsoon climate with two typical rainfall types of long-duration plum rains in spring and short-duration storms in summer (Liu et al., 2016; Duan et al., 2017). The results indicated that the intra-event rainfall types



327 obtained in this paper were consistent with the actual situation of rainfall characteristics in the  
328 study area. The natural rainfall data selected in this paper exhibited good typicality and  
329 representativeness, and the method for classifying intra-event rainfall types was relatively reliable.  
330 However, the intra-storm variations during natural rainfall processes are extremely complex,  
331 which makes them very difficult to quantize (Dunkerley, 2021; Liu et al., 2022). The classification  
332 method used in this study described only one aspect of inter-event rainfall variation, and did not  
333 completely capture all of the properties. Therefore, the development of an available and excellent  
334 index system to quantify intra-event rainfall variability remains a topic requiring an in-depth study  
335 in the future.

336 Figs. 5 and 7 indicate that the surface runoff coefficients and soil loss rates from intra-event  
337 variation patterns were 1.63 to 2.42 times and 15.79 to 39.78 times greater than those from the  
338 uniform pattern, respectively. For soil loss, the results were consistent with previous studies based  
339 on rainfall simulation (Flanagan et al., 1988; Parsons and Stone, 2006; An et al, 2014; Wang et al.,  
340 2017). The studies showed that varying-intensity storms yielded more soil loss than  
341 constant-intensity storms. Similar to simulated rainfall, the intra-event variability for natural  
342 rainfall events played important roles in slope soil erosion. However, studies on the effects of  
343 intra-event rainfall patterns on surface flows had different results. Dunkerley (2012) determined  
344 that uniform events of unvarying intensity yielded the lowest total runoff, the lowest peak runoff  
345 rate and the lowest runoff ratio. The researches found that that varying intensity rainstorms did not  
346 affect total runoff or infiltration (An et al., 2014; Wang et al., 2017). The reasons for the above  
347 results difference were mainly related to factors such as antecedent soil water content, soil types  
348 and topography (Frauenfeld and Truman, 2004; Parsons and Stone, 2006; Alavinia et al., 2019).



349 The uncertainty of intra-event rainfall variation on runoff generation was higher than that of  
 350 sediment yield. In addition, the variation coefficients of soil loss (1.73) were higher than those of  
 351 surface runoff (0.93) on bare land when the rainfall patterns changed (Table 2). The results  
 352 indicated that sediment yields were more sensitive to intra-event rainfall variation than surface  
 353 runoff.

354 **Table 2**

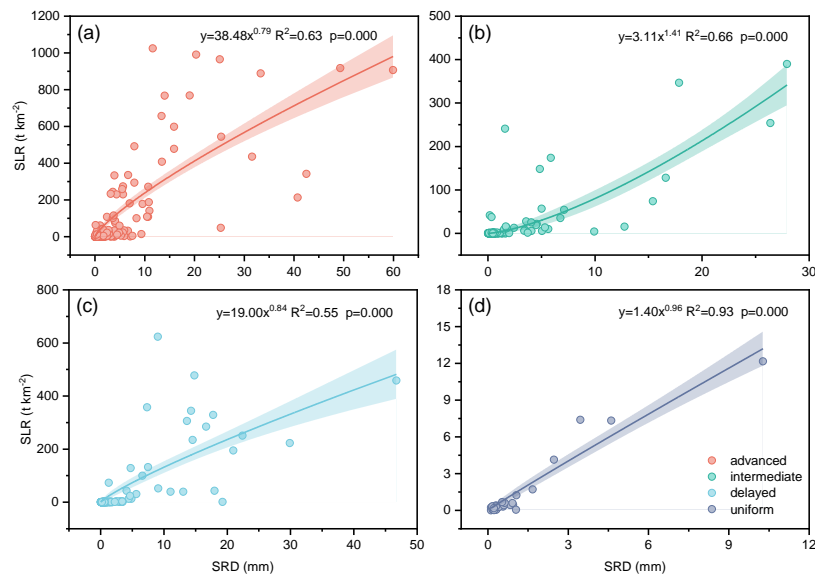
355 The variation coefficients of surface runoff coefficient (ROC), subsurface flow rate (SSL) and soil  
 356 loss rate (SLR) induced by different intra-event rainfall patterns (IRP) and surface cover types  
 357 (SC).

Variation factor	Fixed factor	ROC	SSL	SLR
IRP	Bare land	0.93	2.16	1.73
	Litter cover	0.61	1.45	1.10
	Grass cover	0.65	2.47	1.44
SC	advanced	1.78	2.10	2.81
	intermediate	1.68	2.00	3.00
	delayed	1.78	2.63	3.07
	uniform	1.45	1.79	2.01

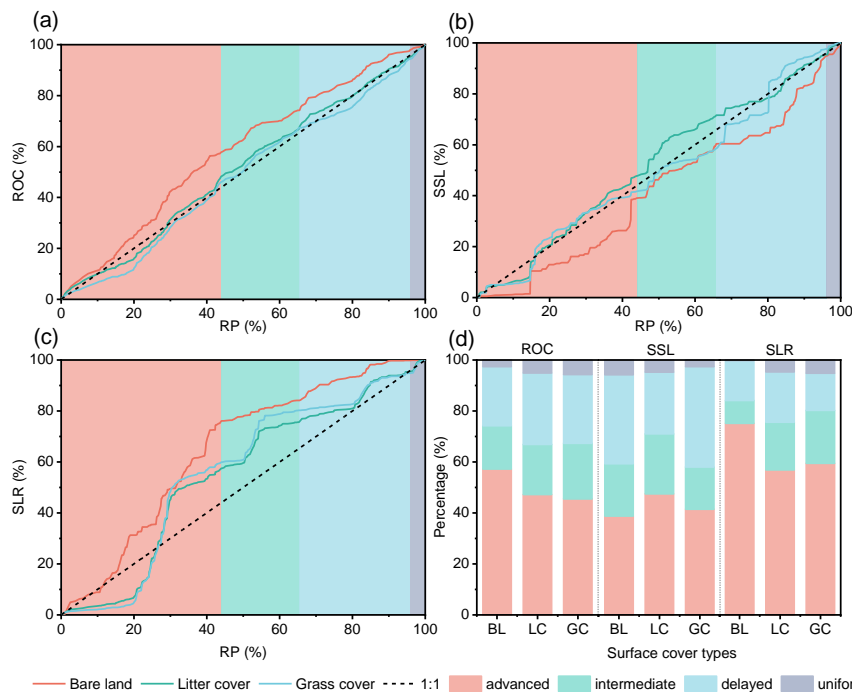
358 As shown in Fig. 8, the power function relationship between surface runoff and soil loss was  
 359 influenced by intra-event rainfall variation. The soil loss rate ranged in the order of advanced  
 360 pattern > delayed pattern > intermediate pattern > uniform pattern under the same surface runoff  
 361 depth. For bare land, the highest surface runoff and soil loss were found in the advanced pattern,  
 362 which were 1.29 to 2.42 times and 2.52 to 39.78 times higher than those in the other three patterns  
 363 (Fig. 5a and 7a). The advanced pattern was the main type for surface flow and soil loss in the bare  
 364 land, with contribution rates of 57.24% and 75.17%, respectively (Fig. 9). All of the above results  
 365 indicated that the events with more rainfall concentrated in the early stages were more favourable  
 366 for surface flow and soil loss. The results were similar to the research of Römken et al. (2001),  
 367 who found that the falling pattern caused more soil loss than the rising pattern. The findings  
 368 contrasted with those of An et al. (2014), Mohamad and Kavian, (2015), and Wang et al. (2016),



369 who reported that the delayed pattern yielded the most soil loss under the same average intensity.  
370 The reason for this phenomenon was possibly the complexity of natural rainfall and the  
371 differences in soil type. In this study, the soil type was clayey red loam with relatively low  
372 permeability. Due to the initially high intensity in the advanced pattern, interrill erosion and  
373 physical crusts were rapidly formed, resulting in decreasing soil infiltration rate and an increase  
374 surface runoff (Liu et al., 2011). The concentrated flow was generated early because of excess  
375 infiltration for the advanced pattern with short duration and heavy intensity (Table 1). Moreover,  
376 in the initial period of rainfall, rapid infiltration quickly increased topsoil moisture and reduced  
377 soil aggregate stability, resulting in increasing the soil erodibility (Le Bissonnais, 2010). The  
378 combined effect of increased surface runoff and decreased soil resistance to erosion inevitably  
379 increased soil erosion. These processes were closely related to antecedent soil water content, soil  
380 texture and soil configuration (Frauenfeld and Truman, 2004; Alavinia et al., 2019). Compared to  
381 the other three patterns, the uniform events with long duration and low intensity led to surface soil  
382 with lower splash erosion and slower seal formation, higher soil infiltration rate and subsequently  
383 less surface runoff and soil loss (Dunkerley, 2012).



384  
385 **Fig. 8** The relationship between surface runoff depth (SRD) and soil loss amount (SLR) under  
386 different intra-event rainfall patterns.



387  
388 **Fig. 9** The relationships between rainfall depth (RP) cumulative percentage and surface runoff  
389 coefficient (ROC), subsurface flow (SSL) and soil loss rate (SLR) cumulative percentages under  
390 different surface cover types. BL, bare land; LC, litter cover; GC, grass cover.



391 Relative to surface runoff and soil loss, the delayed pattern had the greatest average subsurface  
 392 flow, which was 1.26, 1.43, and 2.17 times more than the flow characteristics of the uniform,  
 393 intermediate, and advanced patterns, respectively (Fig. 6). This phenomenon was highly related to  
 394 the rainfall characteristics and slope runoff generation mechanisms of the above intra-event  
 395 rainfall patterns (Wang et al., 2016; Liu et al., 2016). Table 1 clearly shows that the delayed and  
 396 uniform patterns were characterized by long-duration and heavy-intensity rainfall. The duration  
 397 groups of 12-24 h, 24-48 h and >48 h in the delayed pattern accounted for 31.82%, 39.58% and 50%  
 398 of the total rainfall events, respectively. The uniform pattern was only distributed in 6-12 h, 12-24  
 399 h, and 24-48 h groups (Fig. 4). For the delayed and uniform patterns, rainfall intensity in the early  
 400 stage was lower than topsoil infiltration rates. Most of the rainfall infiltrated and accumulated in  
 401 the topsoil layer because of the compact subsoil (Ma et al., 2022a). The subsurface flow under  
 402 constant rain for a long time formed easily owing to excess storage and the lateral slope when  
 403 topsoil moisture reached saturation. In subtropical humid monsoon climate zones, subsurface flow  
 404 could even exceed surface flow and become the primary cause of water loss in some exceptional  
 405 rainfall events (Liu et al., 2016; Duan et al., 2017). Notably, high subsurface flow caused an  
 406 increasing in the soil erosion risk (An et al., 2021). As a result, in terms of soil hydrology and  
 407 erosion process, in addition to advanced rainfall with a short duration and high intensity, more  
 408 attention should be paid to delayed and uniform rainfall events with long duration.

#### 409 4.2 Surface cover regulating the impact of intra-event rainfall variation on water erosion

410 Vegetation effectively increases rainfall infiltration and reduces surface runoff and soil erosion  
 411 (Han et al., 2021; Duan et al., 2022). For each rainfall pattern, long-term continuous in situ  
 412 observations showed that litter cover and grass cover significantly reduced surface runoff and soil



erosion and increased subsurface flow compared to bare land (Fig. 5-7). Reductions in surface runoff and sediment ranged from 88.01 to 91.69% and from 97.80 to 97.95%, respectively, while subsurface flow was 3.55 to 5.92 times greater in surface covered plots (Table 3). The effects of litter cover on reducing surface runoff and soil loss were comparable to those of grass cover. This similarity could be because the two cover types had similar coverage closely relating to surface runoff and sediment loss (Hou et al., 2020). The results confirmed that surface cover with plant litter or grass was effective in reducing surface runoff and erosion, and the influences were not affected by intra-event rainfall variation.

**Table 3**

Average surface runoff coefficient (ROC), subsurface flow rate (SSL) and soil loss rate (SLR) reduction benefit under different intra-event rainfall patterns (IRP).

IRP	ROC (%)		SSL (%)		SLR (%)	
	Litter cover	Grass cover	Litter cover	Grass cover	Litter cover	Grass cover
Advanced	92.29	95.14	-915.44	-546.63	99.75	99.79
Intermediated	89.22	92.16	-563.62	-403.20	99.31	99.34
Delayed	88.69	92.91	-396.94	-286.90	99.58	99.73
Uniform	81.84	86.55	-492.89	-184.46	92.57	92.93
Average	88.01	91.69	-592.22	-355.30	97.80	97.95

The effects of intra-event rainfall variation on surface runoff and sediment loss were strongly influenced by the surface cover. Compared to bare land, the contributions of the advanced pattern to surface flow and soil loss for the surface cover decreased by 9.97-11.69% and 15.68-19.31%, respectively (Fig. 9). The statistical results showed that the variation coefficients of surface runoff and soil erosion for bare land were the highest, and those were more than those for litter cover and grass cover when the rainfall patterns changed (Table 2). The above results indicated that surface cover weakened the impacts of intra-event rainfall variation on surface flow and soil loss. This phenomenon occurred because surface cover effectively reduced splash erosion from rainfall concentration, and led to surface soils without sealing formation, a higher soil infiltration rate and



433 subsequently lower runoff and sediment loss (Wei et al., 2007; Liu et al., 2016; Wang et al., 2020).

434 In addition, the effective buffer layer on the soil surface increased the surface roughness, and

435 delayed the overland flow velocity, thereby reducing the scouring ability of surface runoff on soil

436 (Shi et al., 2012; Fu et al., 2020; Liu et al., 2020). The improvement in the soil anti-erosion ability

437 was another important reason for this phenomenon (Wang et al., 2020; Ma et al., 2022b).

438 Different measures covering the soil surface had varying near-surface characteristics and effects

439 on soil properties along the profile, resulting in distinct soil hydrological responses. The increasing

440 benefit of subsurface flow for litter cover for each rainfall pattern was 1.38 to 2.67 times greater

441 than that of grass cover (Table 3). Due to no difference in surface runoff, more rainfall was

442 converted to soil water storage and deeper infiltration under grass cover than under litter cover for

443 constant rainfall. For long-term coverage of the soil surface, the plant litter was buried by soil

444 particles from water and wind erosion (Hewins et al., 2017). The incorporation of plant litter into

445 the topsoil layer actively impacted soil hydraulic properties such as bulk density, soil infiltration,

446 and saturated hydraulic conductivity (Jordán et al., 2010; Wang et al., 2020). Rainfall infiltration

447 tended to take the form of matrix infiltration, with large amounts of rainfall being stored in the

448 topsoil layer. Because of loose top- compact bottom soil configuration, the topsoil was easily

449 saturated and generated subsurface flow, but rainfall was more difficult to convert into deep soil

450 moisture (Fig. 10b). For grass cover, rainfall infiltration was greater in the form of preferential

451 flow with many root channels (Guo et al., 2019). Before topsoil saturation, rainfall was highly

452 susceptible to rapid infiltration into the subsoil by preferential flow, leading to little subsurface

453 flow and large water storage in the deeper layers (Fig. 10c).



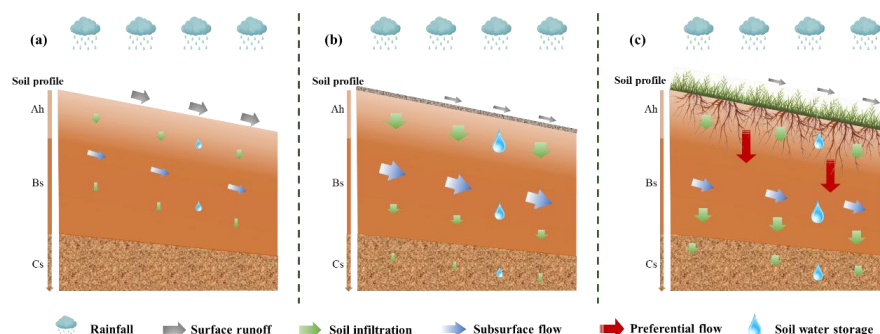


**Fig. 10** Conceptual diagram of the soil hydrological processes under the bare land (a), litter cover (c) and grass cover slopes.

The increasing effects of surface cover on subsurface flow varied among different rainfall patterns. For litter cover and grass cover, the highest increases were observed in the advanced pattern at 915.44% and 546.63%, respectively, which were significantly higher than those in the intermediate, uniform, and delayed patterns (Table 3). As shown in Fig. 9, surface cover increased the contribution rate of the advanced pattern to the subsurface flow from 38.76 to 47.54%. The reason for this phenomenon was that the surface cover increased the soil infiltration capacity and prevented the formation of surface crusts, increasing the amount of rainfall that was concentrated earlier to infiltrate the soil. Concerning subsurface flow variation, the coefficient of variation for litter cover was much smaller than the coefficients for bare land and grass cover (Table 2). The results illustrated how the effects of intra-event rainfall variability on subsurface flow were easily masked by litter cover. This phenomenon occurred due to the strong water absorption of the litter layer, which was an important source for steady water infiltration (Darboux et al., 2002). For the grass cover, the water absorption capacities of the aboveground parts were relatively weak, and rainfall infiltration and subsurface flow were more susceptible to intra-event rainfall changes. This response was particularly observed for events with more rainfall concentrated in the early stages, which tended to form preferential flows.



473 *4.3 Implications and further scopes*

474 Human disturbances played a crucial role in surface runoff and soil erosion intensification. For  
475 example, serious soil disturbance induced by large scale mechanical excavation resulted in  
476 enormous regions of bare soil during agricultural land use (Niu et al., 2021). The inter- and  
477 intra-event variations were important consequences of rainfall changes with global warming  
478 (Dunkerley, 2021b; An et al., 2022). The increase in extreme rainfall frequency and intensity was  
479 the most typical form of expression, and finally water erosion risk was aggravated (Nie et al.,  
480 2020; Shenoy et al., 2022). In this paper, based on long-term in situ observations, the two  
481 measures of surface cover showed very good stability in reducing surface runoff and sediment,  
482 regardless of the inter- and intra-event rainfall variation. In addition, the differences in surface  
483 runoff and soil loss from the inter- and intra-event rainfall changes were weakened by litter cover  
484 or grass cover. The results showed that covering bare soil with plant litter or planted grass can  
485 effectively mitigate the water erosion risk caused by climate change and unreasonable human  
486 activities.

487 The increased risk of drought frequency, duration, and intensity was another important issue  
488 arising from global climate change and anthropogenic impacts. Droughts have severe  
489 environmental and socio-economic influences, especially in countries relying on rain-fed  
490 agricultural production (Sternberg, 2011; Chiang et al., 2021). Storing more precipitation in soil  
491 during the flood season is an effective way to address this hazard, especially to increase deep soil  
492 water storage. Deep soil moisture provided a potential water source for crops utilization during the  
493 dry season (Wu et al., 2021). In this study, surface runoff from the slope was comparable under the  
494 two cover measures, while subsurface flow was greater under litter cover than grass cover. In



495 other words, the grass cover resulted in more soil water storage and deeper permeation than the  
496 litter cover. Moreover, soil water storage was mainly in the topsoil layer for litter cover and in the  
497 subsoil and deeper layers for grass cover. Therefore, to improve soil, crop and water productivity  
498 under rainfed hill ecosystems, there is a great need to adapt single mulching to diversified  
499 mulching measures (Ngangom et al., 2020). For example, double mulching technology involving  
500 plant litter and planted grass can increase shallow and deep soil water storage while reducing  
501 surface runoff and erosion, and mitigate the hazards of agricultural production caused by extreme  
502 climate.

## 503 **5 Conclusion**

504 In this study, 262 natural rainfall events were classified into four intra-event rainfall patterns  
505 (advanced, intermediate, delayed, and uniform) over 11 consecutive years in the red soil region of  
506 China. Three surface cover types including bare land, litter cover and grass cover were selected to  
507 study the response of surface-subsurface flow and soil loss to intra-event rainfall variation. The  
508 advanced pattern was the most frequent rainfall event that had the shortest duration and the  
509 highest intensity. The intermediate pattern was represented by moderate duration and moderate  
510 intensity. The delayed pattern involved the longest duration and highest depth. The uniform  
511 pattern was characterized by long duration and the lowest intensity and frequency.

512 Surface runoff and soil loss in the advance pattern were highest, followed by the delayed,  
513 intermediate, and uniform patterns. Sediment yields were more sensitive to intra-event rainfall  
514 variation compared to surface runoff. However, the subsurface flow was in the order of delayed  
515 pattern > uniform pattern > intermediate pattern > advanced pattern. For all rainfall patterns, bare  
516 land had the highest surface runoff and soil loss. Surface cover significantly reduced surface



runoff and soil erosion by 88.01 to 91.69% and 97.80 to 97.95%, respectively, while subsurface flow increased from 3.55 to 5.92 times. The reduction benefits of litter cover were comparable to those of grass cover. However, compared to bare land, the increasing benefit of subsurface flow for litter cover for each rainfall pattern ranged from 1.38 to 2.67 times that of grass cover. Moreover, surface cover can weaken the influences of intra-event rainfall variation on surface-subsurface flow and soil loss. These findings could enhance the understanding of the impacts of rainfall changes at inter- and intra- event scales on key surface processes such as surface-subsurface flow and soil erosion, and provide a basis for optimizing surface cover measures to effectively respond to extreme disasters caused by global climate change.

#### **Data availability**

The data that support the findings of this study are available from the corresponding author upon request.

#### **Author contributions**

Jian Duan was responsible for the data investigation, analysis, and methodology and completed the original draft of the article. Haijin Zheng and Yaojun Liu conceptualized this research, including conceptualization and methodology, and participated in the review and editing of the writing. Minghao Mo contributed to the data investigation and the review and editing of the writing. Yuejun Song and Jie Yang were involved in writing review and editing.

#### **Competing interests**

The contact author has declared that none of the authors has any competing interests.

#### **Acknowledgements**

This research was supported by the National Natural Science Foundation of China (42107378,



41877084, 42067020) and Science and Technology Project of Jiangxi Province (20212AEI91011,  
 2022KSG01001). We would like to acknowledge the anonymous reviewers, associate editor  
 and editor for their valuable comments and kind assistance on this manuscript.

## References

- Almeida, W.S. de, Seitz, S., Oliveira, L.F.C. de, Carvalho, D.F. de, 2021. Duration and intensity of  
 rainfall events with the same erosivity change sediment yield and runoff rates. *Int. Soil Water  
 Conservat. Res.* 9, 69–75. <https://doi.org/10.1016/j.iswcr.2020.10.004>.
- Alavinia, M., Saleh, F.N., Asadi, H., 2019. Effects of rainfall patterns on runoff and  
 rainfall-induced erosion. *Int. J. Sedim. Res.* 34(3), 270–278.  
<https://doi.org/10.1016/j.ijsrc.2018.11.001>.
- An, J., Zheng, F.L., Han, Y., 2014. Effects of rainstorm patterns on runoff and sediment yield  
 processes. *Soil Sci.* 179(6), 293–303. <https://doi.org/10.1097/SS.000000000000068>.
- An, J., Wu, Y.Z., Wu, X.Y., Wang, L.Z., Xiao, P.Q., 2021. Soil aggregate loss affected by raindrop  
 impact and runoff under surface hydrologic conditions within contour ridge systems. *Soil  
 Tillage Res.* 209, 104937. <https://doi.org/10.1016/j.still.2021.104937>.
- An, J.X., Gao, G.Y., Yuan, C., Pinos, J., Fu, B.J., 2022. Inter- and intra-event rainfall partitioning  
 dynamics of two typical xerophytic shrubs in the Loess Plateau of China. *Hydrol. Earth Syst.  
 Sci.* 26, 3885–3900. <https://doi.org/10.5194/hess-26-3885-2022>.
- Chiang, F., Mazdiyasn, O., AghaKouchak, A., 2021. Evidence of anthropogenic impacts on global  
 drought frequency, duration, and intensity. *Nat. Commun.* 12, 2754.  
<https://doi.org/10.1038/s41467-021-22314-w>.
- Darboux, F., Gascuel-Oudoux, C., Davy, P., 2002. Effects of surface water storage by soil  
 roughness on overland-flow generation. *Earth Surf. Proc. Land.* 27, 223–233.  
<https://doi.org/10.1002/esp.313>.
- Duan, J., Yang, J., Tang, C.J., Chen, L.H., Liu, Y.J., Wang, L.Y., 2017. Effects of rainfall patterns  
 and land cover on the subsurface flow generation of sloping Ferralsols in southern China. *PLoS  
 One* 12, e0182706. <https://doi.org/10.1371/journal.pone.0182706>.
- Duan, J., Liu, Y.J., Wang, L.Y., Yang, J., Tang, C.J., Zheng, H.J., 2022. Importance of grass stolons  
 in mitigating runoff and sediment yield under simulated rainstorms. *Catena* 213, 106132.  
<https://doi.org/10.1016/j.catena.2022.106132>.
- Dunkerley, D., 2012. Effects of rainfall intensity fluctuations on infiltration and runoff: rainfall  
 simulation on dryland soils, Fowlers Gap, Australia. *Hydrol. Process.* 26 (15), 2211–2224.  
<https://doi.org/10.1002/hyp.v26.1510.1002/hyp.8317>.
- Dunkerley, D., 2021. The importance of incorporating rain intensity profiles in rainfall simulation  
 studies of infiltration, runoff production, soil erosion, and related landsurface processes. *J.  
 Hydrol.* 603, 126834. <https://doi.org/10.1016/j.jhydrol.2021.126834>.
- Fang, N.F., Shi, Z.H., Li, L., Guo, Z.L., Liu, Q.J., Ai, L., 2012. The effects of rainfall regimes and  
 land use changes on runoff and soil loss in a small mountainous watershed. *Catena* 99, 1–8.  
<https://doi.org/10.1016/j.catena.2012.07.004>.
- Flanagan, D.C., Foster, G.R., Moldenhauer, W.C., 1988. Storm pattern effect on infiltration, runoff,  
 and erosion. *Trans. Am. Soc. Agric. Eng.* 31 (2), 414–420. <https://doi.org/10.13031/2013.30724>.



- 580 Frauenfeld, B., Truman, C., 2004. Variable Rainfall Intensity Effects on Runoff and Interrill  
 581 Erosion From Two Coastal Plain Ultisols in Georgia. *Soil Sci.* 169, 143–154.  
 582 <https://doi.org/10.1097/01.ss.0000117784.98510.46>.
- 583 Fu, S.H., Mu, H.L., Liu, B.Y., Yu, X.J., Zhang, G.H., Liu, Y.N., 2020. Effects on the plant stem  
 584 arrangement on sediment transport capacity of croplands. *Land Degrad. Dev.* 31 (11),  
 585 1325–1334. <https://doi.org/10.1002/ldr.3512>.
- 586 García-Ruiz, J.M., Beguería, S., Nadal-Romero, E., González-Hidalgo, J.C., Lana-Renault, N.,  
 587 Sanjuán, Y., 2015. A meta-analysis of soil erosion rates across the world. *Geomorphology* 239,  
 588 160–173. <https://doi.org/10.1016/j.geomorph.2015.03.008>.
- 589 GSP, 2017. Global Soil Partnership Endorses Guidelines on Sustainable Soil Management  
 590 <http://www.fao.org/global-soil-partnership/resources/highlights/detail/en/c/416516/>
- 591 Guo, L., Liu, Y., Wu, G.L., Huang, Z., Cui, Z., Cheng, Z., Zhang, R.Q., Tian, F.P., He, H.H., 2019.  
 592 Preferential water flow: Influence of alfalfa (*Medicago sativa* L.) decayed root channels on soil  
 593 water infiltration. *J. Hydrol.* 578. <https://doi.org/10.1016/j.jhydrol.2019.124019>.
- 594 Hammad, A.H.A., Børresen, T., Haugen, L.E., 2006. Effects of rain characteristics and terracing  
 595 on runoff and erosion under the Mediterranean. *Soil Tillage Res.* 87, 39–47.  
 596 <https://doi.org/10.1016/j.still.2005.02.037>.
- 597 Han, T., Lu, H., Lü, Y., Fu, B., 2021. Assessing the effects of vegetation cover changes on resource  
 598 utilization and conservation from a systematic analysis aspect. *J. Clean. Prod.* 293, 126102.  
 599 <https://doi.org/10.1016/j.jclepro.2021.126102>.
- 600 Hewins, D.B., Sinsabaugh, R.L., Archer, S.R., Throop, H.L., 2017. Soil litter mixing and  
 601 microbial activity mediate decomposition and soil aggregate formation in a sandy  
 602 shrub-invaded Chihuahuan Desert grassland. *Plant Ecol.* 218(4), 459–474.  
 603 <https://doi.org/10.1007/s11258-017-0703-4>.
- 604 Hou, G.R., Bi, H.X., Huo, Y.M., Wei, X.Y., Zhu, Y.J., Wang, X.X., Liao, W.C., 2020. Determining  
 605 the optimal vegetation coverage for controlling soil erosion in *Cynodon dactylon* grassland in  
 606 North China. *J. Clean. Prod.* 244, 118771. <https://doi.org/10.1016/j.jclepro.2019.118771>.
- 607 Huff, F.A., 1967. Time distribution of rainfall in heavy storms. *Water Resour. Res.* 3 (4),  
 608 1007–1019. <https://doi.org/10.1029/WR003i004p01007>.
- 609 Jordán, A., Zavala, L.M., Gil, J., 2010. Effects of mulching on soil physical properties and runoff  
 610 under semi-arid conditions in southern Spain. *Catena* 81, 77–85.  
 611 <https://doi.org/10.1016/j.catena.2010.01.007>.
- 612 Le Bissonnais, Y., 2010. Aggregate stability and assessment of soil crustability and erodibility: I.  
 613 Theory and methodology. *European Journal of Soil Science*, 67(1), 11–21.  
 614 [https://doi.org/10.1111/ejss.4\\_12311](https://doi.org/10.1111/ejss.4_12311).
- 615 Liu, J.B., Liang, Y., Gao, G.Y., Dunkerley, D., Fu, B.J., 2022. Quantifying the effects of rainfall  
 616 intensity fluctuation on runoff and soil loss: From indicators to models. *J. Hydrol.* 607, 127494.  
 617 <https://doi.org/10.1016/j.jhydrol.2022.127494>.
- 618 Liu, H.Q., Yang, J.H., Liu, C.X., Diao, Y.F., Ma, D.P., Li, F.H., Rahma, A.E., Lei, T.W., 2020.  
 619 Flow velocity on cultivated soil slope with wheat straw incorporation. *J. Hydrol.* 584, 124667.  
 620 <https://doi.org/10.1016/j.jhydrol.2020.124667>.
- 621 Liu, H., Lei, T.W., Zhao, J., Yuan, C.P., Fan, Y.T., Qu, L.Q., 2011. Effects of rainfall intensity and  
 622 antecedent soil water content on soil infiltrability under rainfall conditions using the run  
 623 off-on-out method. *J. Hydrol.* 396, 24–32. <https://doi.org/10.1016/j.jhydrol.2010.10.028>.



- 624 Liu, Y.J., Yang, J., Hu, J.M., Tang, C.J., Zheng, H.J., 2016. Characteristics of the  
 625 surface–subsurface flow generation and sediment yield to the rainfall regime and land-cover by  
 626 long-term in-situ observation in the red soil region, Southern China. *J. Hydrol.* 539, 457–467.  
 627 <https://doi.org/10.1016/j.jhydrol.2016.05.058>.
- 628 Ma, Y.C., Li, Z.W., Deng, C.X., Yang, J., Tang, C.J., Duan, J., Zhang, Z.W., Liu, Y.J., 2022a.  
 629 Effects of tillage-induced soil surface roughness on the generation of surface–subsurface flow  
 630 and soil loss in the red soil sloping farmland of southern China. *Catena* 213, 106230.  
 631 <https://doi.org/10.1016/j.catena.2022.106230>.
- 632 Ma, J., Li, Z., Ma, B., Wang, C., Sun, B., Shang, Y., 2022b. Response mechanism of the soil  
 633 detachment capacity of root-soil composites across different land uses. *Soil Tillage Res.* 224,  
 634 105501. <https://doi.org/10.1016/j.still.2022.105501>.
- 635 Macedo, P.M.S., Pinto, M.F., Sobrinho, T.A., Schultz, N., Coutinho, T.A.R., Carvalho, D.F. de,  
 636 2021. A modified portable rainfall simulator for soil erosion assessment under different rainfall  
 637 patterns. *J. Hydrol.* 596, 126052. <https://doi.org/10.1016/j.jhydrol.2021.126052>.
- 638 Mohamadi, M.A., Kavian, A., 2015. Effects of rainfall patterns on runoff and soil erosion in field  
 639 plots. *Int. Soil Water Conserv. Res.* 3, 273–281. <https://doi.org/10.1016/j.iswcr.2015.10.001>.
- 640 Montanarella, L., Pennock, D.J., McKenzie, N., Badraou, M., Chude, V., Baptista, I., Mamo, T.,  
 641 Yemefack, M., Aulakh, M.S., Yagi, K., Hong, S.Y., 2016. World’s soils are under threat. *Soil* 2,  
 642 79–82. <https://doi.org/10.5194/soil-2-79-2016>.
- 643 Montgomery, D.R., 2007. Soil erosion and agricultural sustainability. *Proc. Natl. Acad. Sci. U.S.A.*  
 644 104, 13268–13272. <https://doi.org/10.1073/pnas.0611508104>.
- 645 Nearing, M.A., Jetten, V., Baffaut, C., Cerdan, O., Couturier, A., Hernandez, M., Le Bissonnais, Y.,  
 646 Nichols, M.H., Nunes, J.P., Renschler, C.S., Souchère, V., van Oost, K., 2005. Modeling  
 647 response of soil erosion and runoff to changes in precipitation and cover. *Catena* 61, 131–154.  
 648 <https://doi.org/10.1016/j.catena.2005.03.007>.
- 649 Ngangom, B., Das, A., Lal, R., Idapuganti, R.G., Layek, J., Basavaraj, S., Babu, S., Yadav, G.S.,  
 650 Ghosh, P.K., 2020. Double mulching improves soil properties and productivity of maize-based  
 651 cropping system in eastern Indian Himalayas. *Int. Soil Water Conserv. Res.* 8, 308–320.  
 652 <https://doi.org/10.1016/j.iswcr.2020.07.001>.
- 653 Nie, J., Dai, P., Sobel, A.H., 2020. Dry and moist dynamics shape regional patterns of extreme  
 654 precipitation sensitivity. *Proc. Natl. Acad. Sci. U.S.A.* 117, 8757–8763.  
 655 <https://doi.org/10.1073/pnas.1913584117>.
- 656 Niu, Y.H., Wang, L., Wan, X.G., Peng, Q.Z., Huang, Q., Shi, Z.H., 2021. A systematic review of  
 657 soil erosion in citrus orchards worldwide. *Catena* 206, 105558.  
 658 <https://doi.org/10.1016/j.catena.2021.105558>.
- 659 Parsons, A.J., Stone, P.M., 2006. Effects of intra-storm variations in rainfall intensity on interrill  
 660 runoff and erosion. *Catena* 67 (1), 68–78. <https://doi.org/10.1016/j.catena.2006.03.002>.
- 661 Pimentel, D., Terhune, E.C., Dyson-Hudson, R., Rochereau, S., Samis, R., Smith, E.A., Denman,  
 662 D., Reifschneider, D., Shepard, M., 1976. Land degradation: effects on food and energy  
 663 resources. *Science* 194, 149–155.
- 664 Poesen, J., 2018. Soil erosion in the Anthropocene: Research needs. *Earth Surf. Proc. Land.* 43,  
 665 64–84. <https://doi.org/10.1002/esp.4250>.
- 666 Römken, M.J.M., Helming, K., Prasad, S.N., 2001. Soil erosion under different rainfall  
 667 intensities, surface roughness, and soil water regimes. *Catena* 46(2–3):103–123.



- 668 [https://doi.org/10.1016/S0341-8162\(01\)00161-8](https://doi.org/10.1016/S0341-8162(01)00161-8).
- 669 Shenoy, S., Gorinevsky, D., Trenberth, K.E., Chu, S., 2022. Trends of extreme US weather events  
 670 in the changing climate. *Proc. Natl. Acad. Sci. U.S.A.* 119(47), e2207536119.  
 671 <https://doi.org/10.1073/pnas.2207536119>.
- 672 Shi, Z.H., Yue, B.J., Wang, L., Fang, N.F., Wang, D., Wu, F.Z., 2012. Effects of much cover rate  
 673 on interrill erosion processes and the size selectivity of eroded sediment on steep slopes. *Soil*  
 674 *Sci. Soc. Am. J.* 77, 257–267. <https://doi.org/10.2136/sssaj2012.0273>.
- 675 Sternberg, T., 2011. Regional drought has a global impact. *Nature* 472, 169–169.  
 676 <https://doi-org-443--bjmu.jitui.me/10.1038/472169d>.
- 677 Todisco, F., 2014. The internal structure of erosive and non-erosive storm events for interpretation  
 678 of erosive processes and rainfall simulation. *J. Hydrol.* 519, 3651–3663.  
 679 <https://doi.org/10.1016/j.jhydrol.2014.11.002>.
- 680 Tsymbarovich, P., Kust, G., Kumani, M., Golosov, V., Andreeva, O., 2020. Soil erosion: An  
 681 important indicator for the assessment of land degradation neutrality in Russia. *Int. Soil Water*  
 682 *Conservat. Res.* 8, 418–429. <https://doi.org/10.1016/j.iswcr.2020.06.002>.
- 683 Wang, B., Steiner, J., Zheng, F., Gowda, P., 2017. Impact of rainfall pattern on interrill erosion  
 684 process. *Earth Surf. Proc. Land.* 42, 1833–1846. <https://doi.org/10.1002/esp.4140>.
- 685 Wang, L.J., Zhang, G.H., Zhu, P.Z., Wang, X., 2020. Comparison of the effects of litter covering  
 686 and incorporation on infiltration and soil erosion under simulated rainfall. *Hydrol. Process.* 34,  
 687 2911–2922. <https://doi.org/10.1002/hyp.13779>.
- 688 Wang, W.T., Yin, S.Q., Xie, Y., Liu, B.Y., Liu, Y.N., 2016. Effects of four storm patterns on soil  
 689 loss from five soils under natural rainfall. *Catena* 141, 56–65.  
 690 <https://doi.org/10.1016/j.catena.2016.02.019>.
- 691 Wei, W., Chen, L., Fu, B., Huang, Z., Wu, D., Gui, L., 2007. The effect of land uses and rainfall  
 692 regimes on runoff and soil erosion in the semi-arid loess hilly area, China. *J. Hydrol.* 335,  
 693 247–258. <https://doi.org/10.1016/j.jhydrol.2006.11.016>.
- 694 Wu, G.L., Cui, Z., Huang, Z., 2021. Contribution of root decay process on soil infiltration capacity  
 695 and soil water replenishment of planted forestland in semi-arid regions. *Geoderma* 404, 115289.  
 696 <https://doi.org/10.1016/j.geoderma.2021.115289>.
- 697 Zhang, X.C., Norton, L.D., Hickman, M., 1997. Rain pattern and soil moisture content effects on  
 698 atrazine and metolachlor losses in runoff. *J. Environ. Qual.* 26, 1539–1547.  
 699 <https://doi.org/10.2134/jeq1997.00472425002600060013x>.
- 700 Zheng, F.L., Huang, C.H., Norton, L.D., 2004. Effects of near-surface hydraulic gradients on  
 701 nitrate and phosphorus losses in surface runoff. *J. Environ. Qual.* 33(6), 2174–2182.  
 702 <https://doi.org/10.2134/jeq2004.2174>.